Study of the Wind-Induced Dynamic Response for a Parabolic- Trough Solar Collector

Dr. Mauwafak Ali.Tawfik
Machines & Equipments Engineering Department, University of Technology/ Baghdad
Dr. Bahaa.Ibrahim.Kazem
Engineering College, University of Baghdad/ Baghdad
Haider.Hussein.Hamad
Engineering College, University of Baghdad/ Baghdad
Email: Haider hussein2010@yahoo.com

ABSTRACT

In this paper, the dynamic response of parabolic-trough due to wind loading was conducted in different flow field environment and configurations experimentally and numerically. First, Experimental modal analysis (EMA) was performed to evaluate the vibrational characteristics for prototype of parabolic trough that manufactured for this purpose. Direct pressure sensors array were used to measure the pressure values over the parabolic trough model surface due to wind load at different operational attitudes. Then, the dynamic response (displacement) of the parabolic-trough due to measured wind loads (pressure) was measured experimentally and numerically. The numerical solution for dynamic response was performed using the finite element approach. The response of the parabolic-trough to wind loads was evaluated for different wind velocities and different angles of attack. A comparison between these results was made to verify the effect of the angles of attack and wind velocity on the dynamic response. The results showed that the suggested approach gave good indication for evaluating the wind load effect on the dynamic response of parabolic trough the solar collector.

دراسة الاستجابة الديناميكية الناتجة عن الرياح للمجمع الشمسي بشكل القطع المكافئ

الخلاصة

هذا البحث يدرس الاستجابة الديناميكية للمجمع الشمسي بشكل قطع مكافئ الناتجة عن تأثير الرياح في ظروف جريان واوضاع مختلفة عمليا وعدديا. في هذا البحث تمت دراسة الاهتزاز عمليا لايجاد خواص الاهتزاز لنموذج من الصحون المستخدمة كمجمع شمسي صنع لهذا الغرض. تم استخدام متحسسات ضغط مرتبطة بصورة مباشرة لايجاد توزيع الضغط على سطح الصحن الناتجة عن تأثير الريح تحت ظروف تشغيل مختلفة. بعد ذلك تم قيست الاستجابة الديناميكية (الازاحة) للصحن الناتجة عن تاثير الرياح (الضغط) عمليا وعدديا. التحليل العددي انجز باستخدام طريقة العناصر المحددة. تم ايجاد الاستجابة الديناميكية للصحن الناتجة عن سرع ريح مختلفة وبزوايا هجوم مختلفة. تمت المقارنة بين النتائج المختلفة لمعرفة تاثير سرع الرياح وزوايا الهجوم

على الاستجابة الديناميكية للصحن. النتائج اظهرت ان الطريقة المستخدمة تعطي تخمين جيد لتأثير
احمال الرياح على الاستجابة الديناميكية لصحن المجمع الشمسي بشكل القطع المكافئ.

INTRODUCTION

The solar concentrating power systems with light structures and low cost technology are used for processing heat the applications up to 400 C. This could be obtained using a parabolic through collectors (PTCs). A large number of troughs are installed in flat sunny terrains to get optimum performance. At such terrains, the parabolic trough can be subjected to various types of wind loads which can cause a dynamic response to decrease the performance. PTCs are made by bending a sheet of reflective material into a parabolic shape [1].So, in order to analyze the dynamic behavior of the parabolic trough we should deal with the trough as open parabolic cylindrical shell as shown in figure(1).
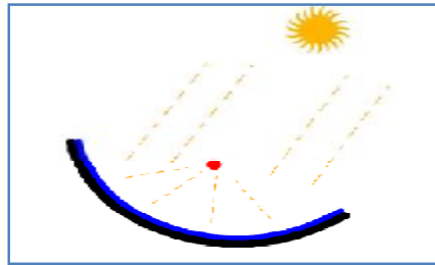

Figure (1): Schematic of a parabolic trough collector.

Vibration of open cylindrical shells has been studied by several researchers in the past few decades. Cheung et al. [2] studied a single curved shell panel and the spline finite strip method was employed in their studies. Al-Jumaily, A.M. [3] used a simplified shell theory to investigate a closed form solutions for the free vibrational characteristics of open profile circular cylindrical shells with different boundary conditions. Suzuki and Leissa [4] studied the free vibrations of circular and non-circular open cylindrical shells with circumferentially varying thickness. Lim et al. [5] investigated the free vibration characteristics of thick open shells based on a three-dimensions elasticity approach. Zhang and Xiang [6] presented a preliminary study on the vibration of open cylindrical shells with intermediate ring supports. M.T. Lates [7] presented the finite elements analysis of the mechanical behavior for three main solar collector tracking systems: for plate, for dish and for trough solar collectors. The study concentrated on the prediction of stresses in solar collectors due to extreme meteorological situations (3cm thick snow layer and 16m/s wind speed) acting on the structure oriented in a horizontal position. A. Miliozzi et.al [8] evaluated wind loads on a parabolic-trough concentrator numerically using the CFD Flotran module of Ansys finite element code. The study concentrated on evaluating the aerodynamics coefficient for the parabolic trough at three wind speed and different angular position. In this study, the dynamic response of parabolic cylindrical shell due to wind loads is obtained numerically and experimentally. To obtain the dynamic response of the structure, the free vibration characteristic was determined first.

Then the dynamic response of parabolic trough due to wind loading was obtained. An artificial wind loading using free jet was utilized on the parabolic

trough with different operational attitudes. The support configuration (boundary conditions) used to support the parabolic trough is chosen to be as those used in the real plant which are designed to satisfy tracking mobility requirement. The geometric properties (shape, dimension and materials) for parabolic trough used in the current study are chosen according to the latest design update of the parabolic trough established at Massachusetts Institute of technology [9]. These dimensions and shape are shown in Figure (2).
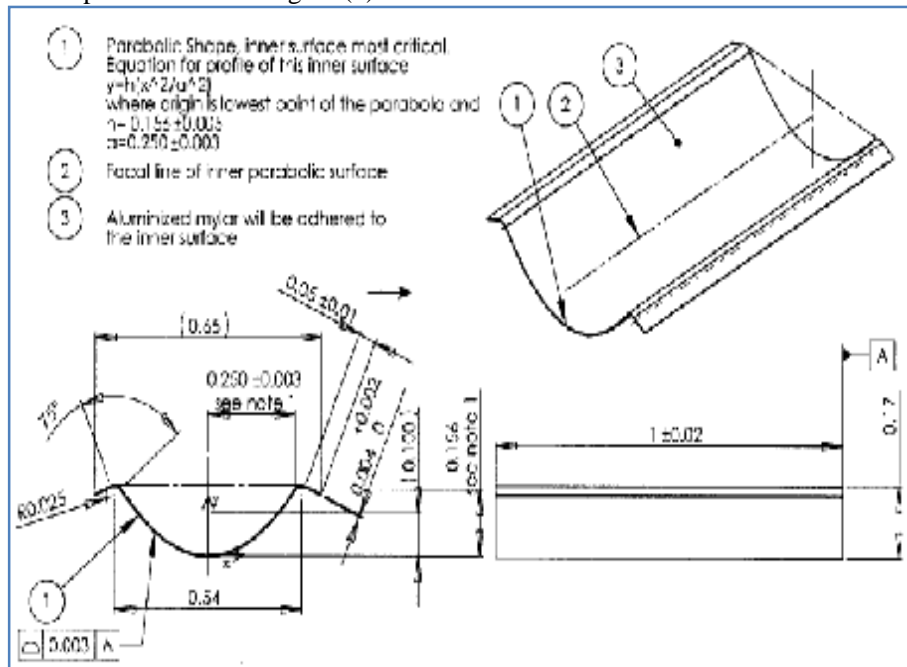

Figure (2): Drawing of 1/10th scale parabolic trough for fiberglass prototype construction [9].

Analytical Solution for Parabolic Cylindrical Shell

An isotropic, open parabolic cylindrical shell with length (L), included curvilinear coordinate (S), linear coordinate (X), thickness (h), midsurface radius ($R_s = a+bs^2$) where (a) is the radius of apex of parabola and (b) is a constant that has to be fitted to the design of interest, Young modulus (E), Poisson′s ratio (μ) and mass density (ρ) is shown in Figure (3). The displacement fields on the midsurface of the open shell with reference to the coordinate system are denoted as u(x, s, t), v(x, s, t) and w(x, s, t) in the x, s and radial directions, respectively. The governing differential equations for the free vibration of a thin open parabolic cylindrical shell based on the shell theory can be written as [10].

3639
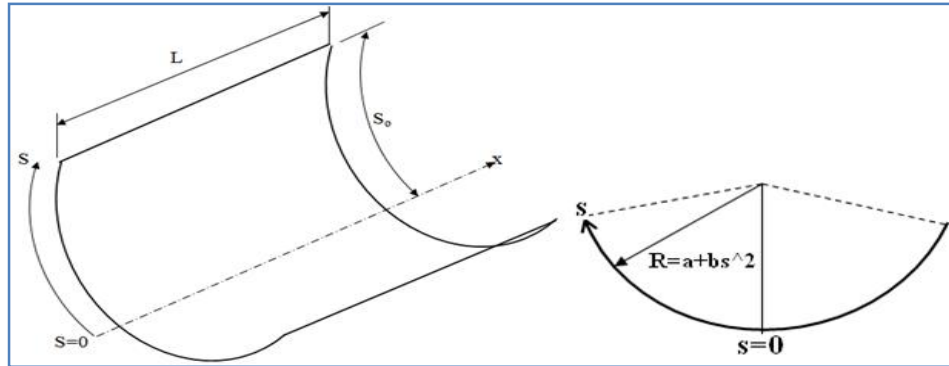
Figure(3): Geometry and coordinate system for an open parabolic cylindrical shell.

$$k \frac{\partial_2 u}{\partial x^2} + \frac{k}{2}(1\text{-}\mu)\frac{\partial_2 u}{\partial s^2} + \frac{k}{2}(1\text{+}\mu)\frac{\partial_2 v}{\partial x \partial s} + k\mu \frac{1}{a+bs^2}\frac{\partial w}{\partial x} + \rho h \omega^2 \, u = 0 \quad \ldots\ldots\ldots\ldots(1)$$

$$\frac{k}{2}(1\text{+}\mu)\frac{\partial_2 u}{\partial x \partial s} + \frac{1}{2}(1\text{-}\mu)(k+\frac{D}{(a+bs^2)^2})\frac{\partial_2 v}{\partial x^2} + k\frac{\partial_2 v}{\partial s^2} + \frac{D}{a+bs^2}\frac{\partial_2}{\partial s^2}\left(\frac{v}{a+bs^2}\right)$$

$$+ k\frac{\partial}{\partial s}\left(\frac{w}{a+bs^2}\right) - \frac{D}{a+bs^2}\frac{\partial_3 w}{\partial s^3} - \frac{D}{a+bs^2}\frac{\partial_3 w}{\partial x^2 \partial s} + \rho h \omega^2 \, v = 0 \quad \ldots\ldots\ldots\ldots\ldots..(2)$$

$$\frac{k\mu}{a+bs^2}\frac{\partial u}{\partial x} + D\frac{\partial_3}{\partial x^2 \partial s}\left(\frac{v}{a+bs^2}\right) + D\frac{\partial_3}{\partial s^3}\left(\frac{v}{a+bs^2}\right) + \frac{k}{a+bs^2}\frac{\partial v}{\partial s}$$

$$-D\left[\frac{\partial_4 w}{\partial x^4} + \frac{\partial_4 w}{\partial x^2 \partial s^2} + \frac{\partial_4 w}{\partial s^4}\right] + \frac{k}{(a+bs^2)^2}w + \rho h \omega^2 \, w = \mathbf{0} \qquad \ldots\ldots\ldots..(3)$$

Where

$k = \frac{Eh}{1-\mu^2}$ is the stretching rigidity and

$D = \frac{Eh^3}{12(1-\mu^2)}$ is the bending rigidity.

The governing differential equations for the free vibration of a thin open parabolic cylindrical shell are complicated equations and the exact solution of these equations is not available for some types of boundary conditions. Approximate solutions such as Rayleigh-Ritz method, Galerkin's method and finite element approach are then used when an exact solution does not exist. In current study, Finite element approach is used to obtain the vibrational characteristic of the structure and experimental work is performed to verify the obtained results.

FINITE ELEMENT MODELING FOR PARABOLIC TROUGH
One of the problems that arising during the design and creation of the complicated structures is a detailed analysis of vibration, strain and stress fields originating in the operating regime. Solution of similar problems taking into account all peculiarities of the construction can be obtained only by means of finite element approach (FEA) modeling [11]. In the current paper, using of FE modeling and analysis of parabolic trough reflector are carried out. Finite element approach is used, first to obtain the free vibrational characteristics of the trough and compare it with experimental results. Then, the dynamic response of the trough due to the

wind load is evaluated. The results of the dynamic response are also compared with those obtained from the experimental dynamic response results. The development modal of the parabolic trough considered the main structural element of the real construction main reflector (thin shells). Eight nodes Structural Shell elements (SHELL281) which is particularly well suited for modeling the curved shells is used. The element has six degrees of freedom at each node, three translations and three rotations [12]. A suitable comparison between the FEA results and the experimental results was achieved.

WIND LOADING

The flow of the fluids such as wind around structures could cause vibrations because of the flow around structures exerts fluctuating forces on the structure. The sources of the fluctuating forces are the natural turbulence in the unsteady flow, vortex shedding near the edges of the structures and the fluid-structure interaction [13]. Fluid models are more tenuous than structures. Since an accurate general model for the fluid forces exerted on an arbitrary bluff structure does not exist, the fluid models rely on extrapolations of the test measurements of the lift, drag or fluctuating surface pressure [14]. In the current study, the measurements of fluctuating surface pressure at many locations on parabolic trough surface are used. Numerical investigation for dynamic response of parabolic trough was carried out using the data of the fluctuating pressure that obtained from the experimental part as input data for the finite element model. Then solving this model to get the response at any point on the surface of the trough. A comparison between the experimental and the numerical results of the response at specific points on the trough were made.

EXPERIMENTAL CONFIGURATIONS
Fabrication of the parabolic trough

The prototype of the parabolic trough used in the experimental work is made with a scale of (1/10) of the original parabolic trough. The profile of the prototype is shown in Figure (2). The prototype that used in this study is made of fiberglass-polyester resin composites. The mechanical properties of the material, including modulus of elasticity, poison's ratio and density are measured. Tensile test experiments (ASTM D638) are performed to obtain the mechanical properties in the principal directions of the material. The results show that the values of the modulus of elasticity in the principal directions are approximately identical. So, we can consider the material as an isotropic. The mechanical properties of trough material are listed in the following table.

Modulus of elasticity (E)	Density (ρ)	Poison's ratio (ν)
5.23 GPa	1460 Kg/m^3	0.416

EXPERIMENTAL MODAL ANALYSIS [EMA]

Experimental modal analysis is a procedure of determining the vibration characterestic which includes the natural frequencies, the damping ratios and the mode shapes. Figure (4) shows the schematic diagram of the experimental apparatus used in the current study. The parabolic trough is attached to the

vibrating base of an electro-mechanical shaker to execute a harmonic motion with a certain amplitude and frequency. Piezoelectric force transducer is attached close to the structure and attached to the shaker using a suitable decoupler (stinger). The force transducer provide signal for the time history of excitation. A piezoelectric accelerometer is attached to the structure to measure the response at various locations of the structure. The signals which come from the force transducer and accelerometer are fed into built in fast Fourier transform (FFT) oscilloscope and then to personal computer interface. Then the two signals fed to signal analysis software (sigview v2.3) to evaluate the frequency response function (FRF) to every pairs of points on the structure. These apparatus are shown in figure (5-a). The prototype is attached to a rigid structure to establish the boundary conditions (c-c, f-f) as shown in Figure (5-b). The frequency response functions are measured at nine points on the structure, (see figure (5-b)).
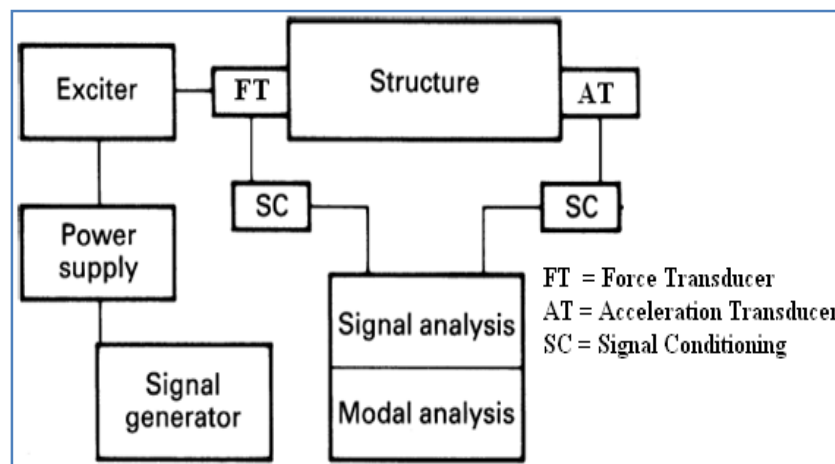

Figure (4) Schematic diagram of the vibration measurement system.

A   B

**Figure(5): a- The vibration measurement configuration for parabolic trough.
b- The fixing of the trough and the points of measurements.**

Wind Load Measurement

   The pressure on the surface of the trough could be varied with the time and location because the nature of the turbulence, separation nears the edges, vortex shedding and the interaction between the fluid and the trough. To get knowledge about the variations of the pressure with time and location, Several pressure tabs are located on the surface of the trough. The locations of the measuring points are shown in Figure (6). The pressure data on the parabolic trough were acquired using multi-pressure system. The system features simultaneous signal samples from (8) individual pressure transducers at default design rate of (12500) samples per second per channel. The signals transmitted from the pressure transducer to (8) channel analog the digital convertor serial communications USB (DAQmx 100 ksa/sec) are connected to controller software (LabVIEW SignalExpress 2010) on a personal computer as shown in figure (7). This system allows digitizing, showing and saving the variations in pressure values with time on the Excel data sheet.
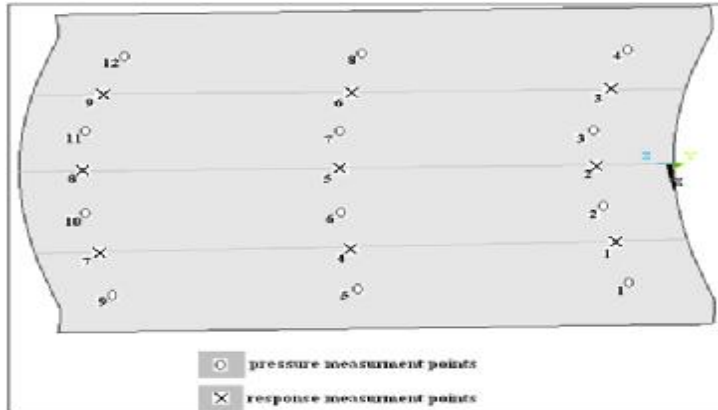
**Figure(6): The locations of the pressure tabs and the
response measuring points.**

The measurements of the pressure are performed at different wind velocities and different angles of attack. The angles of attack used in the current study are (0˚, 45˚, 90˚, 135˚, 180˚, -45˚, -90˚ and-135˚) as shown in Figure (8). The wind velocities used in the current study are (10, 15 and 20 m/s) to evaluate the wind loads corresponding to these velocities. These three wind velocities are repeated at each operational configuration of parabolic trough.

Figure(7): The pressure measuring system configuration.

3644
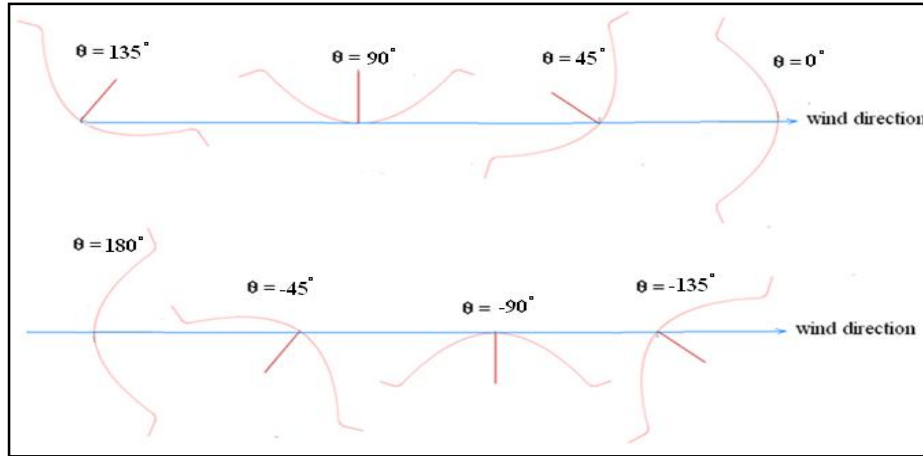
Figure(8): The operational configuration for the parabolic trough with respect to wind flow direction.

RESULT AND DISCUSSION.
### Natural frequencies, damping ratios and mode shapes for the parabolic trough.

The frequency response function (FRF) is measured when the excitation is applied at ith location and the response is measured at jth location where (i,j= 1,2,…9). Each FRF is examined versus the excitation frequency where all the FRFs show a maximum magnitude at approximately specific frequencies which represent the damped natural frequencies of the structure. The magnitudes of FRF at corresponding to damped natural frequencies are differing with each pair of measuring points (ij). Figure (9) shows the typical FRF when the excitation is applied at point (5) and the response is measured at point (1). The first nine damped natural frequencies of the structure are listed in Table (1) obtained by the experimental and the numerical methods and corresponding damping ratios. The mode shape corresponding to each damped natural frequency is evaluated. The relative sign for each modal element is examined by the phase plot between the excitation and the response at each damped natural frequency. Table (2) shows the modal vector corresponding to the first damped natural frequency evaluated from experimental FRF's measurements. It is noted that the modal vector obtained from the experimental work is approximately symmetric about centre line while the numerical solution shows symmetric deformation for the mode shape corresponding to the fundamental damped natural frequency. This discrepancy between the experimental and numerical results is belongs to systematic error in FRF measurement such as noise in signals, inaccuracy in parameters extraction from measurements data and the errors in the signal processing of the measured data. Figure (10) shows the first mode shape obtained by the experimental and the numerical analysis figure (11) shows the first nine mode shapes obtained from the numerical analysis.

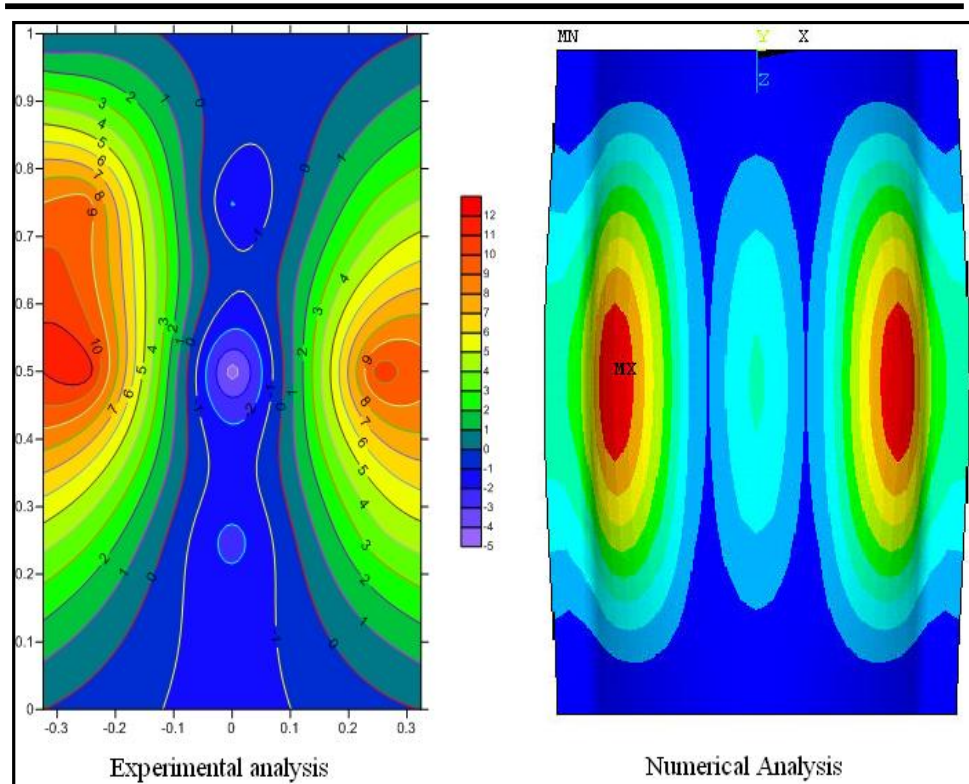**Table(1): the first nine damped natural frequencies.**

NO	Experimental (Hz)	F.E.M (Hz)	discrepancy %	Damping ratio (ζ)
1	61	65.193	6.431	0.024
2	65	72.603	10.472	0.017
3	89	101.02	11.898	0.034
4	92	104.38	7.614	0.015
5	98	108.87	9.984	0.036
6	103	110.23	9.339	0.022
7	121	136.13	11.114	0.018
8	126	139.35	9.58	0.022
9	131	139.43	6.046	0.028

Table(2): The first mode shape obtained by the experimental work.

Modal points	1	2	3	4	5	6	7	8	9
V_1	10.43	-2.447	8.873	11.64	-4.338	10.23	9.352	-2.356	8.658
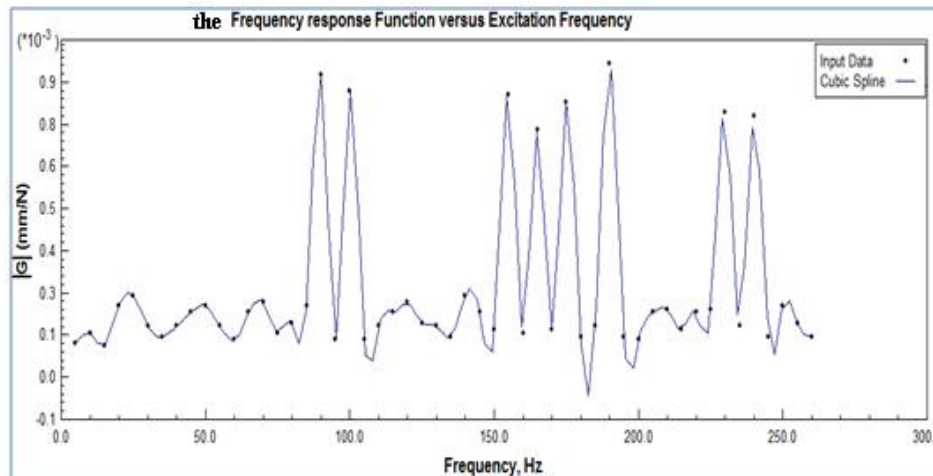
Figure(9): The frequency response function versus excitation frequency.

Experimental analysis   Numerical Analysis

Figure(10): The first mode shape of the (c-c,f-f) trough obtained by the experimental and the numerical analysis.
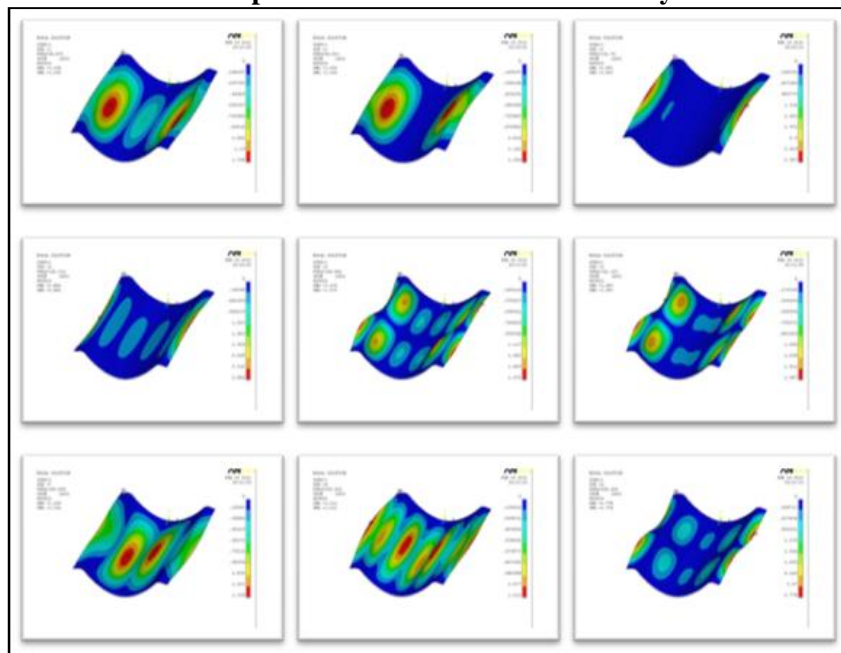
Figure(11): The first nine natural frequencies that obtained from the numerical analysis.

3647

LOCAL MEASUREMENT OF PRESSURE DUE TO WIND

The first observation from the local pressure measurements is that the high local pressure values appear around the edges of the trough for most angles of attack. These high pressures occur at these locations because separations of flow near the edges, vortex formations and the circulation of flow. The presence of high local pressures with high level of fluctuation around the edges leads to high response at these locations. Figure (12) shows typical pressure contour over the trough surface. The second observation is the presence of the pressure gradient over the entire surface of trough. These gradients are very dependent on angles of attack and wind velocity. Also, it is noted that the values of the local pressures increase with the increasing of the wind velocity but these increments of the local pressures are not constant over the entire surface of the trough for specific angle of attack. It also pointed that the values of the maximum local pressures of $(+\theta$ and $-\theta)$ are not identical and it is for $(+\theta)$ always larger than that for $(-\theta)$. For example, the maximum local pressure at $(\theta=+45°)$ is larger than that for $(\theta= -45°)$ and so as for the other angles of attack. This difference can be attributed to the effect of the ground on the velocity distribution over the surface of the trough. For $(\theta= 0°$ and $180°)$, it is pointed that the distribution of the local pressures are approximately symmetric over the whole surface of the trough. This means that the local pressure at point (1) is approximately equal to the local pressure at point (3) at a specific wind velocity. For other angles of attack, the local pressure distribution is not symmetric.
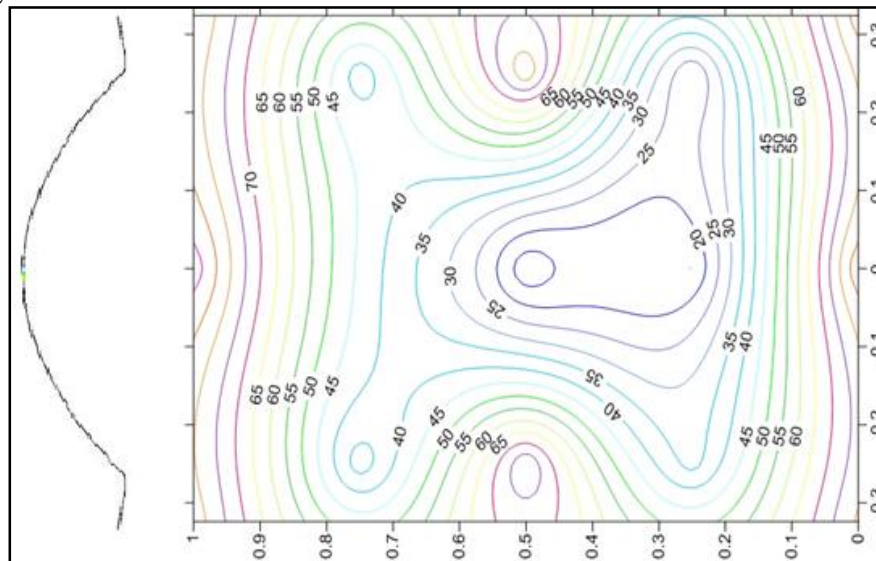

Figure(12): Contour of local pressure over trough surface at wind speed 10m/s
and angle of attack (45°).

Parabolic Trough Dynamic response due to wind load

The dynamic response (displacement) of the parabolic trough due to the wind loading is measured at many points experimentally and numerically. The experimental measurements show that the response is random with time (not harmonic or repeated) and stationary because the changes in the statistical

parameters such as square mean root (S.M.R) do not change with time for specific wind velocity and angle of attack. So, the comparison between the experimental and the numerical results based on (R.M.S) of the response. The comparison between experimental and numerical results of the dynamic response shows that the experimental results always larger than the numerical results because that the actual structure has flexibility more than the numerical model. Also, it appears from the numerical results that the wind excitation within the range used in the current study executes the structure to vibrate and exhibits simultaneous motion.

By this simultaneous motion, all the points on the structure show the same variations with the time but the amplitudes of vibration of points are not same. This simultaneous motion changes with the wind velocity and the angle of attack. Figure (13) shows the displacement response of the structure in a nondimensional form (D/H) where (D) is the displacement response and (H) is the thickness of trough at measuring points (P1-P9) at angle of attack of (θ=45°) and wind velocity of (20m/s). Also, it appears from the experimental and the numerical solutions that the response at points located along the centre line of the trough (s=0) is very small and this response increased when the measuring points approach the edges of the trough. this result also shown in figure (13).This result indicates that the motion of the structure is very constrained by fluctuating aerodynamic forces since the pressure results show that the high pressure regions are located near the edges of the trough and low pressure region is located at the center of the trough. This result is established for most wind velocities and angles of attack.
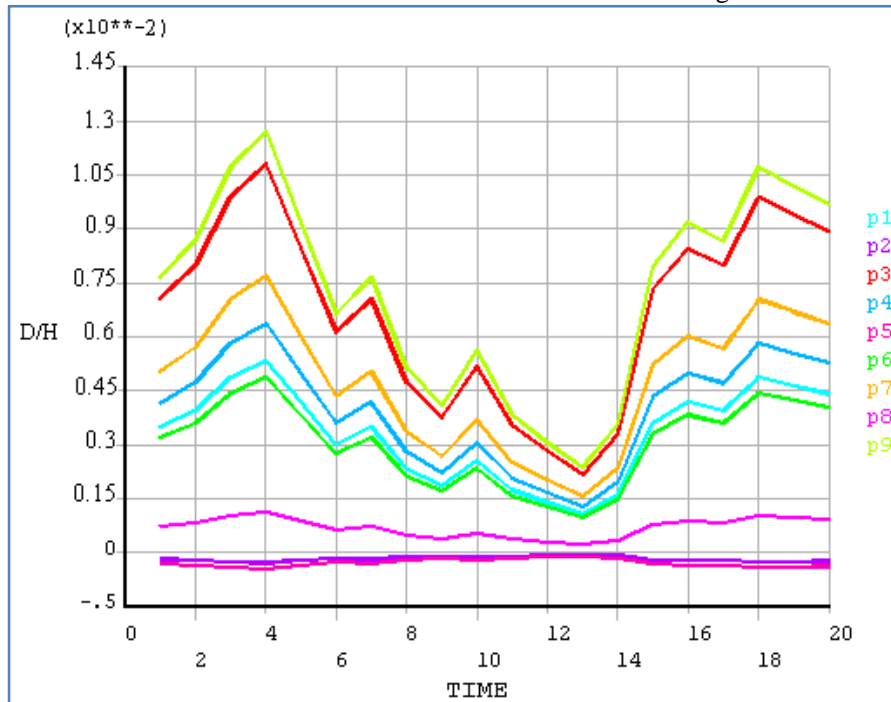
Figure(13): Displacement response at selected locations (P1-P9) at angle of attack (θ=45°) and wind speed (vel=20m/s).

The effect of the angle of attack on the response

To investigate the effect of the angles of attack during wind loading, the response of the points located near the edge of the trough was examined with all angles of attack. The response of points at the centre of the trough which was not examined because of the response at these points is very low as seen in the previous section. Figure (14) shows the response of points (1, 4 and 7) with all angles of attack. For (θ=0˚), although the pressure measurements show a symmetric distribution of the local pressures over the trough surface, the response measurements show that the maximum response occurs at the upper edge of the trough (points 3, 6 and 9). For (θ=45˚, 90˚ and 135˚), the maximum response is also located at the upper edge of the trough (points 3, 6 and 9). These results indicate that for these angles of attack, the response is very constrained by fluctuating of the pressure. For (θ=180˚), the situation is exactly similar to (θ=0˚) except that the direction of the response at points (3, 6 and 9) is opposite to that of (θ=0˚). For (θ= -45˚, -90˚ and -135˚), the response is less than that for (θ=45˚, 90˚ and 135˚). The comparison based on nondimensional ratio (D/H) where D is the absolute maximum value of response and H is the thickness of trough. It is obvious from this figure that the values of responses changes with the angle of attack and reach to its maximum values at angle (θ=45˚ and 90˚).
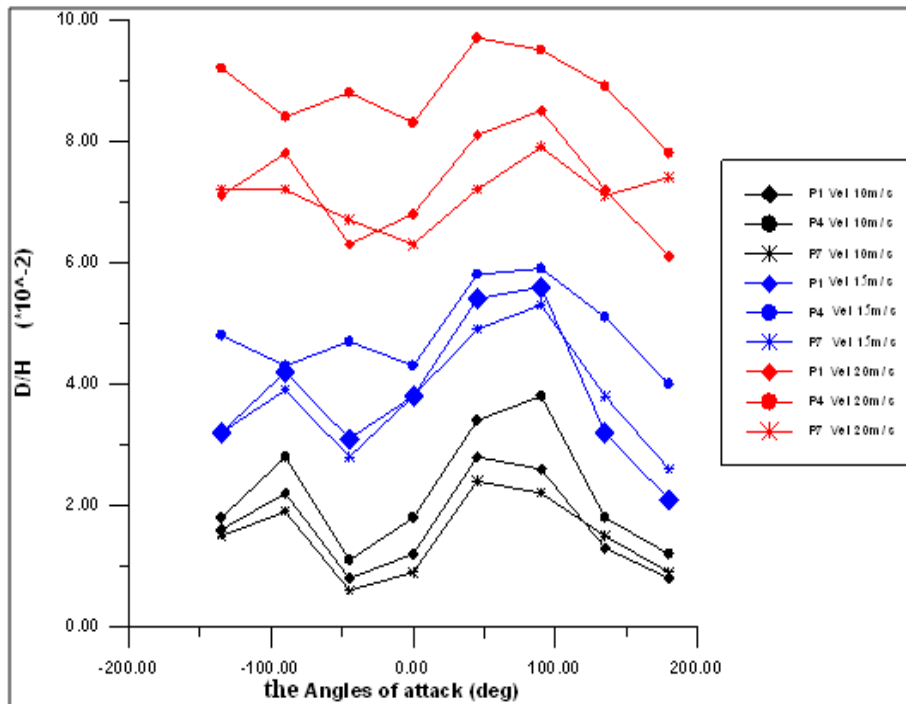

Figure (14) Absolute response value at different angles of attack and wind velocity.

THE EFFECT OF THE WIND VELOCITY ON THE RESPONSE

It is obvious that the increase of the wind velocity leads to an increase in the pressure on the trough surface although the measured pressure is the static pressure. The increase of the wind velocity changes the flow pattern around the trough and increases both dynamic and static pressures. The increase of the pressure around the trough leads to an increase in the response on the trough surface. It is clear that the increase in the response with the increase of the current range of the wind velocity is not high. This result is established for all points on the trough surface and all angles of attack. This indicates that the frequency of vortex shedding near the edges of the trough does not lock in with one of the natural frequencies of the structure at the specified range of wind velocity.

CONCLUSIONS

The new suggested design for parabolic trough shows a high displacement response at the free edges due to the wind load and the response at the points that located along the centre line of the trough (s=0) is very small.

1. The values of the responses change with the angle of attack and reach its maximum values at angle ($\theta=45°$ and $90°$).
2. The increase of the wind velocity leads to a remarkable increase in the response of parabolic trough for all angles of attack.
3. The minimum values of trough surface pressure occur at angle of attack ($\theta=-90°$).
4. The wind excitation specified at this study does not excite the structure to vibrate at its own natural frequency.
5. A high local pressure values appear around the edges of the trough for most angles of attack and the presence of a high local pressures with high level of fluctuating around the edges that leads to high response at these locations.
6. It appears that the wind excitation within the range used in the current study executes the structure to vibrate and exhibit simultaneous motion.

REFERENCES

[1].Soteris A. Kalogirou " Solar thermal collectors and applications" Progress in Energy and Combustion Science, 30 (2004), 231–295.

[2].Cheung, Y.K., Li, W.Y., Tham, L.G., 1980. Free vibration analysis of singly curved shell by spline finite strip method. Journal of Sound and Vibration 128, 411–422.

[3].Al-Jumaily, A.M., 1985. On the free vibration of thin open profile cylindrical shells. American Society of Mechanical Engineers 85- DET-176.

[4].Suzuki, K., Leissa, A.W., 1986. Exact solutions for the free vibrations of open cylindrical shells with circumferentially varying curvature and thickness. Journal of Sound and Vibration 107, 1–15

[5].Lim, C.W., Liew, K.M., Kitipornchai, S., 1998. Vibration of open cylindrical shells: A three-dimensional elasticity approach. Journal of Acoustical Society of America 104, 1436–1443.

[6]. Zhang a, L. Y. Xiang ,2006. Vibration of open circular cylindrical shells with Intermediate ring supports. International Journal of Solids and Structures 43 (2006) 3705–3722

[7]. Lates, M.TMechanical Behavior Analysis with the Finite Element Method of Solar Collectors Tracking Systems. Wseas transaction on applied and theoretical mechanics. Issn 1991-8747, issue 7, volume 3, July 2008.

[8]. Miliozzi,A. D. Nicolini, G. Arsuffi and L. Sipione. Numerical evaluation of Wind action on Parabolic Trough Collectors. 8th. World Congress on Computational Mechanics (WCCM8). 2008.

[9].Stacy L. Figueredo, Parabolic Trough Solar Collectors: Design for Increasing Efficiency, Ph.D thesis, Mechanical engineering department, MIT, 2011.

[10]. soedel. w. "vibration of shells and plates" third edition, Marcel Dekker, Inc, New York, 2004.

[11].Zienkiewicz O.C., Taylor R.L. The Finite Element Method. Butterworth-Heinemann, 2000.

[12].ANSYS theory reference. Twelve edition, 2009.

[13].John D. Holmes, "Wind loading of structures", Spon Press, London 2003.

[14].Robert D. Blevins, "flow-induced vibration", NewYork, 1977.

[15].Clarence W. de Silva, *"Vibration: Fundamentals and Practice"*, Boca Raton: CRC Press LLC, 2000